

Damped Lyman α Surveys and Statistics: A Review

Sandhya M. Rao

Dept. of Physics and Astronomy, University of Pittsburgh, Pittsburgh, PA 15260, USA
 email: rao@everest.phyast.pitt.edu

Abstract.

The discovery of the first damped Lyman alpha (DLA) system in the early 1970s followed by the recognition that DLAs arise in intervening galaxies opened up a new field of galaxy evolution research. These highest HI column density absorption-line systems trace the bulk of the observed neutral gas in the universe, and therefore, have been used as powerful probes of galaxy formation and evolution back to the redshifts of the most distant quasars. The history and progress of DLA research over the past several decades is reviewed here. Larger datasets and deeper surveys, particularly over the last couple of years, have improved our knowledge of the neutral gas content and distribution in the universe at all observable redshifts, including the present epoch. New results on the statistics of DLAs at $z < 1.65$ from our HST-UV surveys are presented and discussed in the context of recent results at $z = 0$ and at high redshift. We find that $\Omega_{DLA}(z > 0)$ remains roughly constant to within the uncertainties; the $z = 0$ value of the neutral gas mass density, Ω_g , is a factor of ≈ 2 less than Ω_{DLA} . The DLA incidence, $n(z)$, undergoes rapid evolution between redshifts 5 and 2, but is consistent with the no-evolution curve in the current concordance cosmology for $z \lesssim 2$. We also show that if the local Schmidt law relating surface density of gas and star formation rate (SFR) is valid at the DLA redshifts, then the DLA SFR density is too low for them to provide a significant contribution to the cosmic star formation history (SFH) at $z \gtrsim 1$. This implies that the DLAs are unlikely to be the same population as the star forming galaxies (i.e., the Lyman break and sub-millimeter galaxies) that dominate the SFH of the high redshift universe. We suggest that this discrepancy and the DLA “missing metals” problem could be the result of missing very high column density gas due to its very small absorption cross section.

Keywords. (galaxies:) surveys, quasars: absorption lines, galaxies: statistics

1. Introduction

The first published spectrum of a damped Lyman α (DLA) system, the $z = 2.309$ absorber towards PHL 957 by Lowrance et al. (1971, 1972), was quickly followed by Beaver et al.’s (1972) independent observation of this object and their interpretation that the strong absorption line might be due to radiation damping from very high column density HI. They showed that the line profile was consistent with a column density of $N(HI) = 2 \times 10^{21}$ atoms cm^{-2} , and noted its similarity to Ly α absorption features along lines of sight to Galactic stars (Savage & Jenkins 1972). Serendipitous discoveries of DLAs towards the quasars Q1331+170, PKS 1157+014, and PKS 0528–250 were reported shortly thereafter (Carswell et al. 1975; Wright et al. 1979; Smith et al. 1979). The discovery of DLAs in the early 1970s in combination with the realization that Ly α forest and narrow metal absorption lines arise in intervening material (Wagoner 1967; Bahcall & Spitzer 1969; Lynds 1971; Weymann et al. 1979; Sargent et al. 1980), led to a whole new approach to the study of galaxy evolution. By tracking absorption line properties with redshift, it was now becoming possible to explore the evolution of gaseous structures in

the universe. DLAs are the highest column density neutral hydrogen absorption lines seen in quasar spectra ($N(HI) \geq 2 \times 10^{20} \text{ cm}^{-2}$), and consequently, have been described as harboring the bulk of the neutral gas in the universe. Thus, barring any selection effects, tracking their properties as a function of redshift directly traces the cosmic evolution of neutral gas in the universe, and since cold neutral gas is a requirement for subsequent star formation, DLAs were soon recognized as important probes of galaxy formation and evolution (Wolfe, Turnshek, Smith, & Cohen 1986). As we describe below, Art Wolfe and collaborators were the first to exploit the potential of DLAs as cosmological probes, and in the early 1980s, began the first systematic search for DLAs.

Prior to the deep imaging surveys of the last decade, DLAs were the only tracers of galaxies at high-redshift. A DLA system was also considered to be an unbiased probe since its detection was independent of the luminosity of the absorbing galaxy, and therefore, DLA-selected samples were thought to be more representative of the galaxy population. The detection of a DLA system only required the presence of a background quasar of sufficient brightness so that its spectrum could be obtained. Moreover, the strong line with damping wings characteristic of a DLA system could be detected in low-resolution spectra with signal-to-noise ratios not much greater than a few. In other words, they were ideally suited for searches through spectroscopic surveys of quasars.

2. DLA Surveys: A brief history

Since the redshifted Ly α line can be observed with groundbased telescopes only for redshifts $z > 1.65$, initial DLA studies were restricted to this regime. Redshifted 21 cm observations of radio loud quasars have also been used to detect large columns of neutral gas in absorption (see Briggs 1999 for an excellent review). Until the advent of UV telescopes, 21 cm absorbers along the line of sight to radio loud quasars were the only known high $N(HI)$ systems below redshift 1.65. Discovery of the first redshifted 21 cm absorption line was reported by Brown & Roberts (1973) towards 3C 286 at $z = 0.692$, not long after the first optically discovered DLA, in a blind survey towards 100 (radio loud) quasars. The DLA towards 3C 196 was also discovered in this survey. Several more were detected towards quasars that had optically-identified low-ionization absorption lines of MgII (Briggs & Wolfe 1983; see Briggs 1988 for a summary). By the early 1980s the pace of DLA discoveries was picking up, but it was clear that surveys were required for DLAs to become useful as statistical probes of neutral gas in the universe. In this section, we describe the progress of DLA studies beginning with optical surveys. It was also obvious that since our end point for galaxy evolution was all around us at $z = 0$, the neutral gas distribution at the present epoch could be used to anchor the evolutionary properties of galaxies observed in the distant universe. Rao & Briggs (1993) made the first attempt to describe the neutral gas distribution at $z = 0$ in a framework for comparison with high redshift DLA studies. In §2.2, we describe this and subsequent $z = 0$ surveys for “DLA” gas. Finally, in §2.3, we present results from surveys for $z < 1.65$ DLAs, the most recently explored redshift regime.

2.1. Optical surveys for DLAs

The Lick DLA Survey was the first systematic search for DLA candidates at redshift $z \sim 2$ (Wolfe et al. 1986). Wolfe et al. characterized the survey as a search for high redshift HI disks, motivated by the fact that DLAs had HI column densities comparable to those found in the Milky Way and in nearby spiral galaxies. The similarities to HI disks extended to their 21 cm properties, i.e., low spin temperatures, high 21 cm optical depths, and low velocity dispersions. The DLAs also showed low-ionization metal-line transitions

such as MgII, FeII, CII, SiII, OI, etc., characteristic of cold clouds in the Milky Way's ISM. The survey included 68 quasars whose spectra were obtained at Lick Observatory at 10 Å resolution. This resulted in 47 absorption lines tagged as DLA candidates in a total redshift path of $\Delta z = 55$. While this was an unexpectedly high incidence of DLAs given the then known incidence of Ly α forest systems (Sargent et al. 1980), follow-up higher resolution spectroscopy (1-2 Å) confirmed 15 bona fide DLAs (Turnshek et al. 1989; Wolfe et al. 1993). This led to the first determination of the incidence of DLA systems, i.e., the number of DLAs per unit redshift. They found $dn/dz = 0.29 \pm 0.07$ at $\langle z \rangle = 2.5$.

This was followed by a larger survey of 100 additional quasars by Lanzetta et al. (1991). Including results from the Lick survey, they found 38 confirmed DLAs in 156 spectra over the redshift range $1.6 < z < 4.1$ and a redshift path of $\Delta z = 155$. With this larger DLA sample, they were able to determine for the first time the key statistical properties that are now routinely used to characterize the evolution of neutral gas, namely, the redshift number density $dn(z)/dz$ [or $n(z)$], the cosmological neutral gas mass density $\Omega_g(z)$,[†] and the column density distribution $f(N)$ for the DLAs. Any theory of galaxy evolution could now be constrained by the observed properties of the neutral gas distribution in the universe. Lanzetta et al. found that the redshift number density could be expressed as a power law $n(z) = n_0(1+z)^\gamma$ with $\gamma = 0.3 \pm 1.4$, which implied that the incidence of DLAs did not evolve with redshift in the non- Λ cosmology that was assumed at the time. They also found that $\Omega_g(z = 2.5) \approx 1 \times 10^{-3}$ was comparable to the mass density of stars in present-day spiral galaxies, and that it did not evolve over the redshifts probed by the survey. Their $f(N)$ distribution was a power law, $f(N) \propto N^{-\beta}$, with $\beta = 1.67$, and showed an excess of systems above the DLA threshold in comparison to the extrapolated power-law distribution of lower $N(HI)$ systems.

Shortly thereafter, Wolfe et al. (1995) described results from spectroscopy of 228 quasars drawn from the Large Bright Quasar Survey. Their statistical sample now included 58 confirmed DLAs at $z > 1.65$ in a redshift path length of over 300. In contrast to the Lanzetta et al. (1991) result, they found that Ω_g decreased with decreasing redshift, and interpreted this evolution as due to depletion from star formation. In addition, they modelled the evolution in the $f(N)$ distribution as being due to star formation in randomly oriented disks and found agreement with the observations if the SFRs followed the standard Schmidt-Kennicutt law seen in nearby galaxies.

The next advancement in DLA studies from the ground occurred when surveys were extended to higher redshifts. As high redshift quasars became more numerous, so did high redshift DLAs; Storrie-Lombardi et al. (1996a,b), Storrie-Lombardi & Wolfe (2000), and Péroux et al. (2001, 2003) extended this work beyond $z = 4$. Storrie-Lombardi & Wolfe compiled a list of 81 DLAs in the redshift interval $1.65 < z < 4.69$; they found that Ω_g was consistent with being constant for $2 < z < 4$ and marginally consistent with a decline at $z > 4$. Péroux et al. discovered an additional 26 new DLAs, 15 at $z > 3.5$, in their survey of 66 $z \gtrsim 4$ quasars. The highest redshift DLA now stood at $z = 4.46$. Péroux et al. also concluded that only 55% of the neutral gas mass at $z > 3.5$ was in DLAs and that the remaining was contained in Lyman limit and sub-DLA systems with HI column densities $10^{19} < N(HI) < 2 \times 10^{20} \text{ cm}^{-2}$. Their result that the total neutral gas mass is conserved over redshifts $2 < z < 5$ led them to suggest that the $z \approx 3.5$ turnover in Ω_g was a signature of the epoch of formation and initial collapse of DLAs.

With the advent of the Sloan Digital Sky Survey (SDSS) and its database of tens of thousands of quasar spectra, the next logical step was to mine it for DLAs. Prochaska

[†] $\Omega_g = 1.3\Omega_{HI}$, where the factor 1.3 corrects for a neutral gas composition of 75% H and 25% He by mass.

& Herbert-Fort (2004) used the SDSS Data Release 1 to find 71 DLA systems in 1252 quasar spectra at a mean redshift of $z \approx 2.5$. Contrary to the result of Péroux et al., they found that Lyman limit systems contribute less than 15% to Ω_g at $z > 3.5$. This conclusion was based on the detection of 6 new DLAs at $z > 3.5$, half of which have $N(HI) > 1 \times 10^{21} \text{ cm}^{-2}$. However, as noted by the authors themselves, the SDSS is most sensitive to DLA redshifts between 2.1 and 3, and the statistical uncertainties beyond $z = 3.5$ are still too high to make a definitive statement about the relative contributions of DLAs and sub-DLAs to the highest redshift values of Ω_g . Prochaska & Herbert-Fort also found that $n(z)$ is consistent with previous estimates, and that Ω_g decreases with decreasing redshift from $z \sim 4$ to $z \sim 2$ with a possible decline beyond $z \sim 4$. However, all of the data points in their figure 5 are within $\sim 1\sigma$ of each other, implying that Ω_g is constant within this redshift range. As we show in §2.3, the low redshift data are consistent with this interpretation. Now, with their larger SDSS DR3 sample in which they detect over 700 DLAs beyond $z = 2.1$, Prochaska et al. (2005) report evidence for a statistically significant decline in Ω_g from $z \sim 4$ to $z \sim 2$. The reader is referred to J. Prochaska's contribution in these proceedings for details on their new results.

Fall & Pei (1989) first suggested that dust in high column density absorbers would influence the statistics of DLAs. The concern was that optically selected quasar samples would miss DLAs due to the reddening and dimming caused by foreground DLA host galaxies (see also Pei et al. 1999). To better evaluate this effect, Ellison et al. (2001) conducted a survey for DLAs towards radio-selected quasars and obtained spectra of all quasars regardless of their optical magnitude. They found that at the mean redshift of their sample, $\langle z \rangle = 2.4$, both n_{DLA} and Ω_{DLA} were only marginally higher than those measured using optically selected samples. Based on the uncertainties in their measurements, which were dominated by sample size, they concluded that Ω_{DLA} could be no more than a factor of two higher than that derived from optical surveys, and that there was no hidden population of DLAs that was being missed in optical surveys. The effects of dust and other biases that might affect DLA statistics will be discussed further in §4. See Turnshek et al. (2005, these proceedings) for more on DLA selection effects.

2.2. The HI distribution at $z = 0$

The first attempt to describe the HI distribution at the present epoch in a form suitable for comparison with DLAs was made by Rao & Briggs (1993) and Rao (1994) who used HI 21 cm emission observations of a complete sample of nearby spiral galaxies to estimate $f(N)$. The 27 galaxies used in the study included all galaxies with optical diameters greater than 7' that were in the declination range observable at Arecibo. They also excluded galaxies in the local group. This Arecibo survey (Briggs et al. 1980) was initiated to explore the distribution of HI in the outskirts of local galaxies with the primary aim of determining the extent of local galaxy halos. The results were then used to interpret quasar absorption line properties. For example, Briggs et al. argued that the lack of detectable HI beyond 2-3 Holmberg radii meant that local galaxies could not reproduce the observed high-redshift MgII absorption line statistics. A decade later, we used these same data on the radial HI distribution of local galaxies to calculate $f(N, z=0)$ as described in Rao & Briggs (1993). In brief, if $\langle A(M, N) \rangle \Delta N$ is the mean cross-sectional area subtended by gas with HI column density between N and $N + \Delta N$ in a galaxy of magnitude M , then

$$f(N) = \frac{c}{H_0} \frac{\sum \Phi(M) \langle A(M, N) \rangle \Delta N \Delta M}{\Delta N}.$$

Here, $\Phi(M)$ is the luminosity function of gas-rich galaxies and is used to normalize $f(N)$. Since the optical luminosity of each galaxy in the sample was known and its radial $N(HI)$ distribution was measured, $\langle A(M, N) \rangle \Delta N$, the area averaged over all inclinations, could be determined. A comparison with the $\langle z \rangle = 2.5$ results of Lanzetta et al. (1991) showed that $f(N, z=0)$ was systematically lower than $f(N, z=2.5)$, and $n(z=0)$, which is the integral of $f(N)$ over all DLA column densities, was a factor of ≈ 5 lower than $n(z=2.5)$. The cosmological mass density of HI, Ω_{HI} , which is proportional to $\int N f(N) dN$, was in agreement with other estimates of the $z=0$ mass density of neutral gas (e.g., Fall & Pei 1993), and was a factor of 3 less than the $z = 2.5$ value. Thus, we had found clear evidence for evolution of neutral gas properties to the present epoch.

However, the local galaxy luminosity function as determined prior to 1993 did not include gas-rich galaxies that are now known to occupy the low-luminosity tail of the galaxy luminosity function. The overall normalization might have been underestimated as well. This offset manifests itself in the values derived for $f(N)$, $n(z)$, and Ω_{HI} . Additionally, the small sample and the large Arecibo beam size meant that improvements could be made (and were necessary) over this initial study. Moreover, the question of whether optically luminous galaxies contained all the HI was still being debated, and the possibility that HI clouds with no optical counterpart could contribute to the HI mass and cross section in the local universe was not completely discounted. To investigate this and to determine $f(N)$ more accurately, many blind HI surveys were launched in the 1990s. The Arecibo HI Strip Survey (AHISS; Sorar 1994; Zwaan et al. 1997), the Arecibo Slice survey (Spitzak & Schneider 1998), the Arecibo Dual Beam Survey (Rosenberg & Schneider 2000), the Parkes all sky southern survey, HIPASS, (Zwaan et al. 2003, 2005; Ryan-Weber et al. 2003), and most recently, the Westerbork Synthesis Radio Telescope (WSRT) survey discussed by M. Zwaan in these proceedings have dramatically improved our knowledge of the HI distribution at the present epoch. Apart from determining $f(N)$, $n(z)$, and Ω_{HI} very accurately, these surveys showed convincingly that all of the neutral gas at the present epoch was accounted for by galaxies included in the optical luminosity function. Minchin et al. (2003), with HIDEEP – a 20 times more sensitive survey than HIPASS in a smaller region of sky – also found that all their HI detections had optical counterparts. This survey’s limits, $N(HI) \approx 4 \times 10^{18} \text{ cm}^{-2}$ and $M(HI) = 4 \times 10^5 \text{ M}_\odot$, were the highest sensitivity limits achieved thus far. Thus, the consensus now is that there are no lurking HI giants or dwarfs in the local universe. While the HI mass density and cross-section are dominated by the high surface brightness, HI rich galaxies, Minchin et al. (2004) showed that low surface brightness galaxies (LSBs) contribute 30% to the HI mass density and 40% to the HI cross-section at the present epoch. This is very different from what was assumed in the initial study of Rao & Briggs (1993), and as Zwaan (this proceedings) also asserts, is completely consistent with the high fraction of LSBs identified as DLA host galaxies at low redshift (e.g., Rao et al. 2003).

2.3. The UV regime: $z < 1.65$

Since the Ly α line falls in the UV for redshifts $z < 1.65$, this most recent 70% of the age of the universe remained hidden until IUE and HST. The need for DLA surveys in the UV is illustrated in Figure 1 where Ω_{DLA} is plotted as a function of time. (We now refer to Ω_g as Ω_{DLA} to specify the cosmological neutral gas mass density measured using DLAs. This change in notation is important because, as we discuss in §4, there is reason to believe that DLAs do not trace all the neutral gas in the universe.) As discussed above, both the optical, high-redshift and 21 cm, $z = 0$ regimes have been serviced by all-sky surveys, namely, the SDSS and HIPASS. While an all-sky UV spectroscopic survey does not exist, and is unlikely, far-fetched, and wishful thinking on our part, we have, nevertheless, been

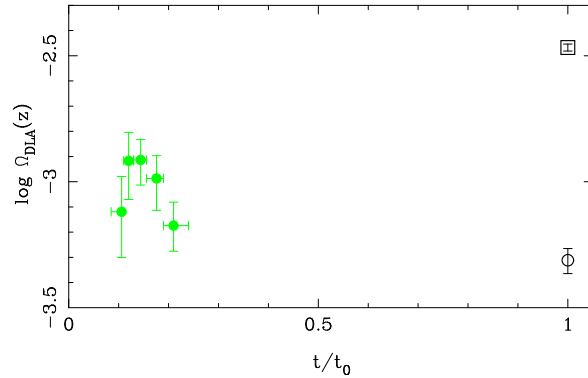


Figure 1. The log of Ω_{DLA} as a function of time (for the “737” cosmology: $h = 0.7$, $\Omega_M = 0.3$, $\Omega_\Lambda = 0.7$) with t_0 representing $z = 0$. The open circle is Ω_g at $z = 0$ from Zwaan et al. (2005) and the open square is the mass density of luminous matter at the present epoch from Panter et al. (2004). The high redshift (early times) data points are from Prochaska & Herbert-Fort (2004). The large gap in time accessible only by UV surveys for Ly α illustrates the importance of the $z < 1.65$ redshift regime for DLA evolution studies.

making incremental progress towards determining DLA statistics in this regime. The first concerted effort to obtain a large sample of UV spectra of quasars was made by the IUE satellite. Kinney et al. (1991) and Lanzetta, Turnshek, & Sandoval (1993) published a total of 260 IUE quasar and AGN spectra, which were subsequently used by Lanzetta, Wolfe, & Turnshek (1995) to estimate the incidence of DLAs in the UV. The IUE spectra proved to be unreliable, and follow-up spectra of the DLA candidates with HST confirmed only one of the four DLAs that were used to determine DLA statistics (Turnshek & Rao 2002). Two were shown to not be DLAs, while the fourth was not observed with HST. Additionally, one system which was later shown to be a DLA did not satisfy the IUE sample’s DLA criterion.

DLAs at low redshift were turning out to be very rare objects, and sample sizes had to be increased several fold to be able to get reasonably good statistics. Traditional blind surveys were not yielding useful results. In fact, the HST QSO absorption line Key Project found only one DLA in a redshift path of $\Delta z = 49$ (Jannuzi et al. 1998). In Rao (1994) and Rao, Turnshek, & Briggs (1995), we used IUE and HST archival spectra to search for DLAs in previously-known, optically-identified MgII systems. This was similar to the selection procedure used by Briggs & Wolfe (1983) to find 21 cm absorbers towards radio-loud quasars. Since low ionization metal lines are always seen along neutral gas sightlines in the Milky Way and in high-redshift DLAs, they act as tracers of high column density HI. Moreover, the MgII doublet, $\lambda\lambda 2796, 2803$, is accessible for $z > 0.11$ in optical quasar spectra. Beginning in the late 1980s, several groups conducted MgII absorption line surveys and discovered many more MgII systems than were available for the initial 21 cm searches of Briggs & Wolfe (Lanzetta, Turnshek, & Wolfe 1987; Tytler et al. 1987; Sargent et al. 1988, 1989; Caulet 1989; Steidel & Sargent 1992, SS92). The SS92 survey, which was the largest, included 107 systems and resulted in the determination of the incidence of MgII systems as a function of redshift and MgII $\lambda 2796$ rest equivalent width. Thus, if a MgII sample was selected appropriately and the fraction of DLAs in this sample could be determined, then the MgII statistics could be used to calculate DLA statistics. We found 4 candidate DLAs in available IUE and HST archival data, and were able to place an upper limit on the values of $n(z)$ and Ω_{DLA} at $z = 0.8$ by using this method.

In order to increase the low-redshift DLA sample, we obtained UV spectra of a sample of 60 additional MgII systems with HST-FOS in Cycle 6. The sample of MgII lines for our initial archival and Cycle 6 surveys was culled from the literature (Rao & Turnshek 2000, RT00) and had a rest equivalent width limit of $W_0^{\lambda 2796} > 0.3 \text{ \AA}$. The total sample of MgII systems with UV Ly α information now included 82 systems of which 12 were DLAs. With these results, we showed that Ω_{DLA} was high at redshifts $0.1 < z < 1.65$, consistent with a constant value for the neutral gas mass density from $z \approx 4$ to $z \approx 0.5$. This was primarily due to the high fraction of $N(HI) > 10^{21} \text{ cm}^{-2}$ systems found in the survey. Our results also suggested that systems with both MgII $\lambda 2796$ rest equivalent width, $W_0^{\lambda 2796} > 0.5 \text{ \AA}$ and FeII $\lambda 2600$ rest equivalent width, $W_0^{\lambda 2600} > 0.5 \text{ \AA}$ had a 50% chance of being a DLA. Based on this result, we conducted a similar survey of 54 MgII systems in 37 quasars with HST-STIS in Cycle 9. Most of these satisfied the strong MgII-FeII criterion for DLAs. Twenty seven had useful UV spectra and four of these were DLAs. The DLA towards Q1629+120 was discovered in this survey and was reported in Rao et al. (2003). The others are reported in Rao, Turnshek, & Nestor (2005a, RTN05). The strong MgII-FeII criterion has since been modified using our new HST Cycle 11 survey - see below. Meanwhile, using the same technique, Lane (2000) surveyed radio loud quasars for 21 cm absorption corresponding to 62 MgII systems with the WSRT, and derived a similar result for Ω_{DLA} at $z < 1.65$ (see Lane & Briggs 2001).

With the number of quasar UV spectra increasing rapidly in the HST archives, it became possible to conduct a UV survey for MgII at redshifts $0 < z < 0.15$. Churchill (2001) used 147 HST archival quasar/AGN spectra to obtain a total redshift search path of 18.8, and found 4 strong MgII systems. For $W_0^{\lambda 2796} > 0.6 \text{ \AA}$, he derived $dn/dz = 0.22_{-0.09}^{+0.12}$ at $\langle z \rangle = 0.06$, consistent with the extrapolation of dn/dz to lower redshifts for $W_0^{\lambda 2796} > 0.6 \text{ \AA}$ from Nestor (2004). All four quasars now have HST UV spectra that include redshifted Ly α at the absorber redshifts. Three of the four have sub-DLA column densities and no information is available for the fourth due to an intervening Lyman limit system (Churchill 2001; Rao HST GO program 9382; Keeney et al. 2005). Thus, the number of DLAs in this sample is ≤ 1 . This gives a 1σ upper limit to the DLA redshift number density of $n(z = 0.06) \leq 0.19$. While this result does not offer significant constraints, it is, nevertheless, consistent with the data points at $z = 0$ and at low redshift (see §3).

3. New results at low redshift

Further progress could only be made with a dramatic increase in sample size. The SDSS sample of quasars, which numbered in the thousands when this phase of our MgII-DLA project began, presented an unprecedented leap in the number of available survey quasars. The previous largest MgII survey by Steidel and Sargent (SS92) used a sample of 103 quasars; the SDSS Early Data Release included nearly 4000. Nestor (2004) used SDSS-EDR quasar spectra to search for MgII systems with the aim of quantifying the statistical properties of a large MgII sample (Nestor, Turnshek, & Rao 2005, henceforth NTR05) and to conduct follow-up work to search for DLAs. In Cycle 11 (PID 9382), we targeted a sample of 83 MgII systems with $W_0^{\lambda 2796} \gtrsim 1 \text{ \AA}$ in 75 SDSS quasars. There were an additional 16 weaker MgII systems observable in the same set of spectra. Overall, useful UV information was obtained for 88 systems, 25 of which are DLAs. For details of the sample and the selection criteria used to include MgII systems in the survey, the reader is referred to RTN05. In total, we now have 197 $z < 1.65$ MgII systems with $W_0^{\lambda 2796} > 0.3 \text{ \AA}$ for which UV observations of the Ly α line have been obtained. Forty one of these are DLAs.

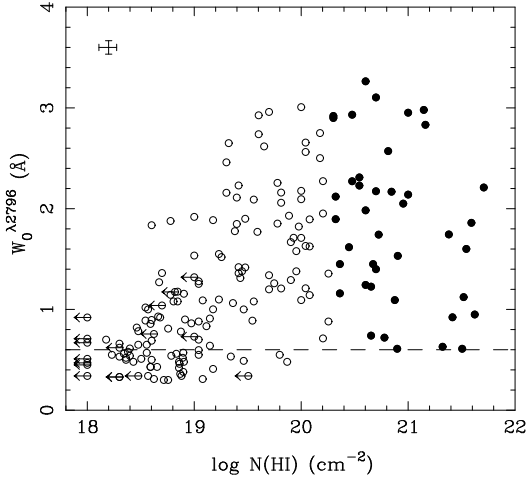


Figure 2. Plot of $W_0^{\lambda 2796}$ vs. $\log N(HI)$ from RTN05. Filled circles are DLAs with $N(HI) \geq 2 \times 10^{20} \text{ cm}^{-2}$. Arrows are upper limits in $N(HI)$. Typical uncertainties are given by the error bars in the top left corner.

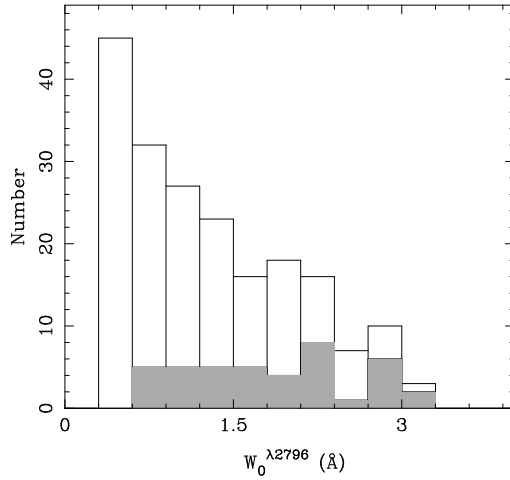


Figure 3. Distribution of MgII $\lambda 2796$ rest equivalent widths, $W_0^{\lambda 2796}$. The gray histogram represents systems that are DLAs. Note that there are no DLAs in the first bin, i.e., for MgII $W_0^{\lambda 2796} < 0.6 \text{ \AA}$. The number of DLAs is roughly constant for $W_0^{\lambda 2796} > 0.6 \text{ \AA}$, implying that the fraction of MgII systems that are DLAs increases with increasing $W_0^{\lambda 2796}$. See RTN05.

3.1. Metal line and HI correlations

Since the systems in our sample were selected based on the rest equivalent width of MgII $\lambda 2796$, $W_0^{\lambda 2796}$ and $N(HI)$ measurements exist for all 197 systems. MgII $\lambda 2803$, the weaker member of the doublet, was also measured for all systems, while the FeII $\lambda 2600$ and MgI $\lambda 2852$ lines were measured for only a subset. Here, we explore correlations among metal line rest equivalent widths and HI column density. Figure 2 is a plot of $W_0^{\lambda 2796}$ versus $\log N(HI)$. We note that the upper left region of the figure is not populated implying that systems with $W_0^{\lambda 2796} > 2.0 \text{ \AA}$ always have HI column densities $N(HI) > 1 \times 10^{19} \text{ atoms cm}^{-2}$. Figure 3 gives the distribution of MgII $W_0^{\lambda 2796}$; the DLAs form

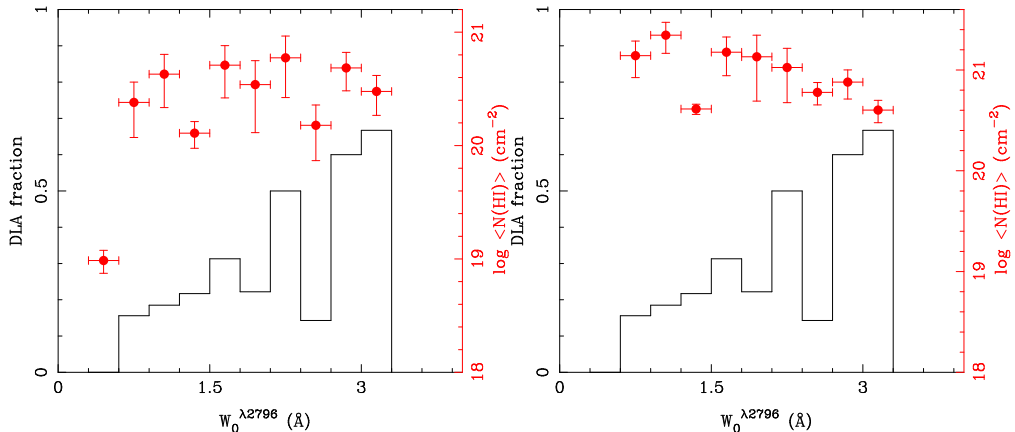


Figure 4. Both histograms show the fraction of MgII systems that are DLAs as a function of MgII $W_0^{\lambda 2796}$, with the scale shown on the left axis. The solid circles are the logarithm of the mean HI column density in each bin for all observed MgII systems in the left panel and only for the DLAs in the right panel. The scale is shown on the right.

the gray histogram. It is noteworthy that there are no DLAs with $W_0^{\lambda 2796} < 0.6 \text{ \AA}$.† In addition, the number of DLAs remains roughly constant for $W_0^{\lambda 2796} > 0.6 \text{ \AA}$. As a consequence, the fraction of systems that are DLAs increases with increasing $W_0^{\lambda 2796}$. This is shown as a histogram in Figure 4; the y-axis on the left gives the fraction of DLAs as a function of $W_0^{\lambda 2796}$. We also plot the mean HI column density in each bin as solid circles with the scale shown on the right. Upper limits are assumed to be detections. The left panel includes all observed MgII systems and the right panel includes only the DLAs. The vertical error bars are standard deviations in the mean and are due to the spread of $N(HI)$ values in each bin, and the horizontal error bars indicate bin size. For the MgII systems, there is a dramatic increase of a factor of ≈ 36 in the mean HI column density from the first to the second bin, beyond which $\langle N(HI) \rangle$ remains constant within the errors. For systems with $0.3 \text{ \AA} \leq W_0^{\lambda 2796} < 0.6 \text{ \AA}$, $\langle N(HI) \rangle = (9.7 \pm 2.2) \times 10^{18} \text{ cm}^{-2}$, and $\langle N(HI) \rangle = (3.5 \pm 0.7) \times 10^{20} \text{ cm}^{-2}$ for systems with $W_0^{\lambda 2796} \geq 0.6 \text{ \AA}$. The right panel shows a trend for decreasing DLA column density with $W_0^{\lambda 2796}$. The reasons for this are not obvious, but are likely to be due to small number statistics (see Figure 2), a real physical effect or a selection effect that is not yet understood (Turnshek et al. 2005).

Figure 5a is a plot of $W_0^{\lambda 2796}$ vs. $W_0^{\lambda 2600}$ for systems with measured values of $W_0^{\lambda 2600}$, including upper limits. In RT00 we found that 50% of the 20 systems (excluding upper limits and 21 cm absorbers) with both $W_0^{\lambda 2796} > 0.5 \text{ \AA}$ and $W_0^{\lambda 2600} > 0.5 \text{ \AA}$ are DLAs. Now, with the expanded sample that includes 106 systems in this regime, we find that 36% are DLAs. The dashed line is a least-squares fit with slope $b = 1.36$. We note that DLAs do not populate the top left region of the diagram where the $W_0^{\lambda 2796}$ to $W_0^{\lambda 2600}$ ratio is $\gtrsim 2$. In fact, if the sample is restricted to systems with $W_0^{\lambda 2796}/W_0^{\lambda 2600} < 2$, all but one of the DLAs from Figure 5a are retained, the outliers in the top left region are excluded as are most systems in the lower left corner of the plot. Figure 5b shows this truncated sample; the slope of the least-squares fit does not change significantly. We find $b = 1.43$. The only DLA that has been eliminated is the one with the smallest value of $W_0^{\lambda 2600}$. However,

† Only one known DLA has lower metal-line rest equivalent widths. The 21 cm absorber at $z = 0.692$ towards 3C 286 has $W_0^{\lambda 2796} = 0.39 \text{ \AA}$ and $W_0^{\lambda 2600} = 0.22 \text{ \AA}$ (Cohen et al. 1994). None of the 21 cm absorbers are included in our analysis here because they are biased systems (see RT00).

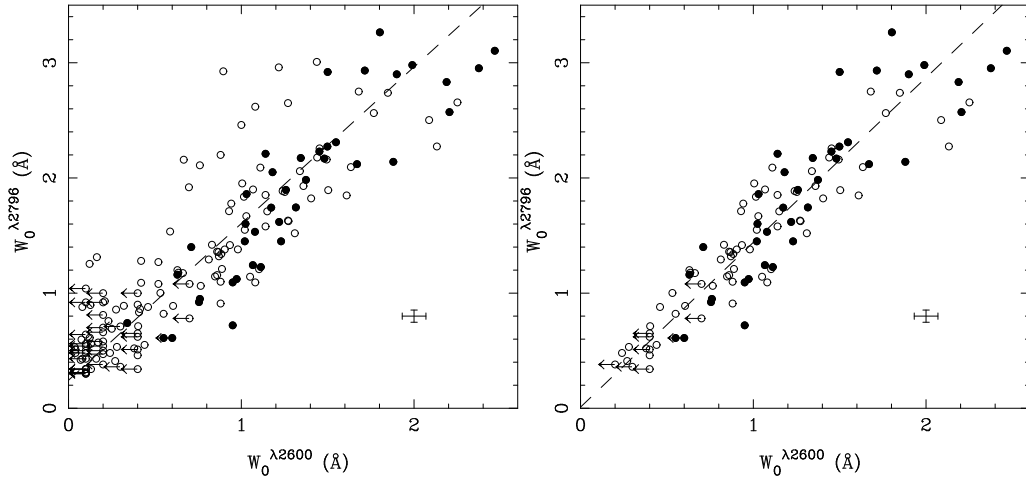


Figure 5. *Left, a:* Plot of $W_0^{\lambda 2796}$ vs. $W_0^{\lambda 2600}$ for all MgII systems that have measured values of $W_0^{\lambda 2600}$. Filled circles are DLAs. Typical error bars are shown in the lower right corner. The dashed line is the best fit linear correlation with slope $b = 1.36$. *Right, b:* Plot of $W_0^{\lambda 2796}$ vs. $W_0^{\lambda 2600}$ for systems with $W_0^{\lambda 2796}/W_0^{\lambda 2600} < 2$. Non-DLAs in the upper left and lower left regions of the diagram have been eliminated and the correlation is tighter than what is seen in Figure 5a. Also, 38% of all systems are DLAs regardless of the values of $W_0^{\lambda 2796}$ and $W_0^{\lambda 2600}$; we believe this to be a more robust predictor of the presence of DLAs in MgII-FeII systems. The slope of the best fit linear correlation is $b = 1.43$. Results are from RTN05.

given the measurement errors for this system, its $W_0^{\lambda 2796}/W_0^{\lambda 2600}$ ratio is within 1σ of 2. This also implies that a system with metal line ratio $W_0^{\lambda 2796}/W_0^{\lambda 2600} > 2$ has nearly zero probability of being a DLA. For this truncated sample with $W_0^{\lambda 2796}/W_0^{\lambda 2600} < 2$, but no restrictions on the individual values of $W_0^{\lambda 2796}$ or $W_0^{\lambda 2600}$, 38% are DLAs. In addition, all known 21 cm absorbers, including the $z = 0.692$ system towards 3C 286 mentioned above, have $W_0^{\lambda 2796}/W_0^{\lambda 2600} < 2$. Thus, the $W_0^{\lambda 2796}/W_0^{\lambda 2600}$ ratio is a more robust predictor of the presence of DLAs.

This result is shown more dramatically in Figure 6. The ratio $W_0^{\lambda 2796}/W_0^{\lambda 2600}$ is plotted as a function of $N(HI)$ in Figure 6a. Ratios above 5 are not shown for clarity. These are mainly confined to $\log N(HI) < 19.2$ with only one system above this column density at $\log N(HI) = 19.6$. The DLAs populate the region of the plot where $1 \lesssim W_0^{\lambda 2796}/W_0^{\lambda 2600} \lesssim 2$; the two outliers lie within 1σ of this range. A plot of the ratio $W_0^{\lambda 2796}/W_0^{\lambda 2600}$ vs. MgI $W_0^{\lambda 2852}$ for systems with measured values of $W_0^{\lambda 2852}$, including upper limits, is shown in Figure 6b. Again, the DLAs are confined to the region where $1 \lesssim W_0^{\lambda 2796}/W_0^{\lambda 2600} \lesssim 2$, but span the entire range of $W_0^{\lambda 2852}$. The two systems outside the range $1 \lesssim W_0^{\lambda 2796}/W_0^{\lambda 2600} \lesssim 2$ from Figure 6a do not have any information on $W_0^{\lambda 2852}$. We find that 9 out of the 11 systems with $W_0^{\lambda 2852} > 0.8 \text{ \AA}$ are DLAs. We also note that systems with $W_0^{\lambda 2796}/W_0^{\lambda 2600} \gtrsim 2$ are likely to have low values of $W_0^{\lambda 2852}$.

For completeness, we also plot $W_0^{\lambda 2600}$ vs. $\log N(HI)$ in Figure 7a and $W_0^{\lambda 2852}$ vs. $\log N(HI)$ in Figure 7b. There is no obvious trend in these distributions except for the fact that the upper left regions of the plots are not populated. There are no high rest equivalent width, low HI column density systems. This is not a selection effect since column densities as low as 10^{18} cm^{-2} can often be easily measured. As is the case for $W_0^{\lambda 2796}$, this implies that systems with $W_0^{\lambda 2600} \gtrsim 1 \text{ \AA}$ or $W_0^{\lambda 2852} \gtrsim 0.5 \text{ \AA}$ generally have HI column densities $N(HI) > 10^{19} \text{ cm}^{-2}$. Below this fairly sharp boundary, metal-line rest equivalent widths span all values of HI column density.

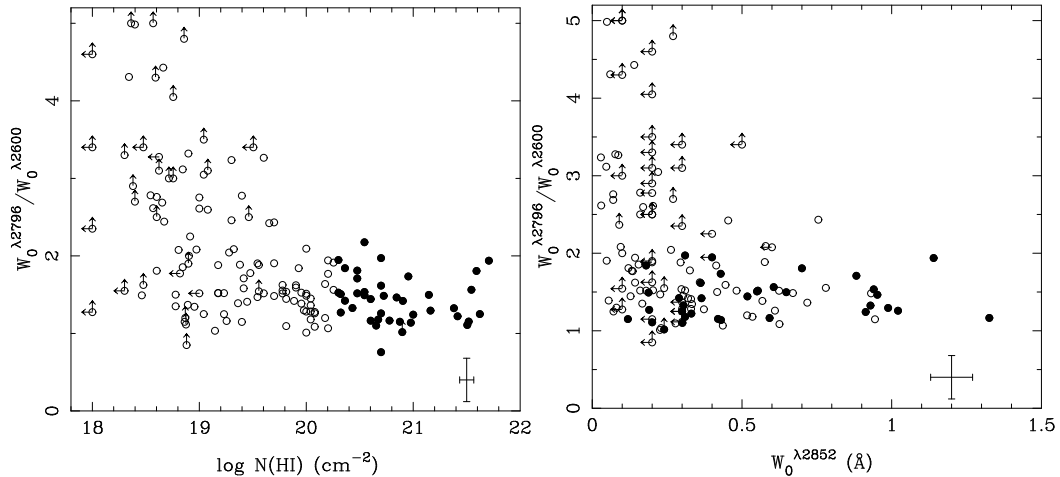


Figure 6. *Left, a:* Plot of $W_0^{\lambda 2796}/W_0^{\lambda 2600}$ vs. $N(HI)$. Systems with $W_0^{\lambda 2796}/W_0^{\lambda 2600} > 5$ are not shown for clarity; all of these have $\log N(HI) < 19.6$. The DLAs are confined to the region of the plot where $1 \lesssim W_0^{\lambda 2796}/W_0^{\lambda 2600} \lesssim 2$. *Right, b:* Plot of $W_0^{\lambda 2796}/W_0^{\lambda 2600}$ vs. MgI $W_0^{\lambda 2852}$. Solid circles are DLAs. Typical error bars are shown in the lower right corner. Again, the DLAs are confined to the region where $1 \lesssim W_0^{\lambda 2796}/W_0^{\lambda 2600} \lesssim 2$, but span the entire range of $W_0^{\lambda 2852}$.

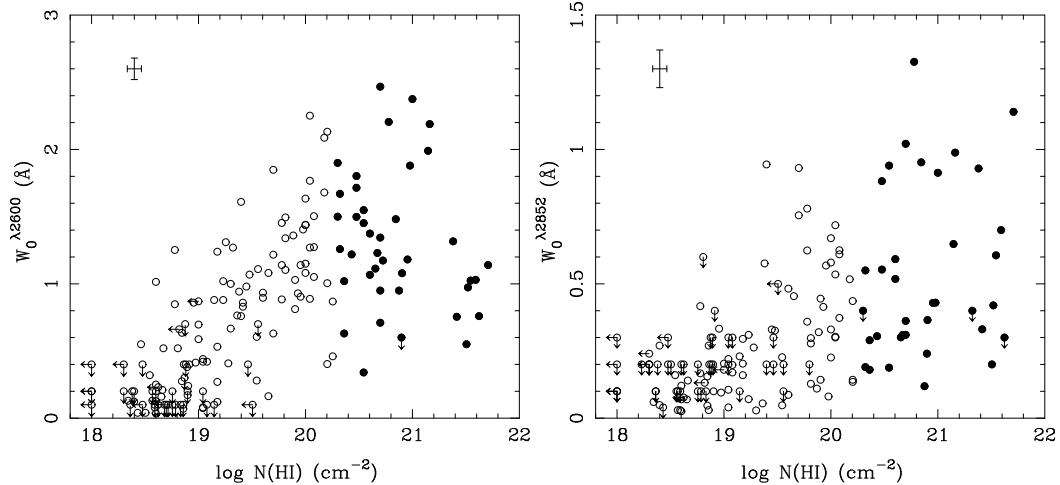


Figure 7. *Left, a:* Plot of $W_0^{\lambda 2600}$ vs. $\log N(HI)$. Arrows indicate upper limits. Typical uncertainties are given by the error bars in the top left corner. *Right, b:* Plot of $W_0^{\lambda 2852}$ vs. $\log N(HI)$. Arrows indicate upper limits. Typical uncertainties are given by the error bars in the top left corner.

3.2. Interpretation of Absorption Characteristics

How can these trends be interpreted? Apart from the upper envelopes in Figures 2 and 7, there is no correlation between metal-line rest equivalent width and HI column density. Since the metal lines are saturated, the rest equivalent width is more a measure of kinematic velocity spread and not column density. High resolution observations of MgII absorption lines have shown that the stronger systems break up into many components (e.g., Churchill et al. 2003), and span velocity intervals of up to 400 km/s. Turnshek et al. (2005) show line equivalent widths in velocity units of $\gtrsim 800$ km/s in the strongest systems found in the SDSS. These highest equivalent width systems may arise in galaxy

groups; however, the more common systems like those in our DLA survey are more likely to arise in clouds that are bound in galaxy-sized potentials. A DLA is observed if one of the clouds along the sightline happens to be cold (less than a few 100 K), dense, and with a velocity dispersion of a few 10s of km/s. The more the number of clouds along the sightline, the higher the probability of encountering a DLA. This would explain the higher fraction of DLAs among large $W_0^{\lambda 2796}$ systems and the lack of a correlation between $W_0^{\lambda 2796}$ and $N(HI)$. Only very rarely would a sightline intersect a single cloud resulting in small $W_0^{\lambda 2796}$ and high $N(HI)$, as in the 3C 286 system described in §3.1. This probabilistic approach to explain metal-line and HI strengths in high- $N(HI)$ absorbers was also proposed by Briggs & Wolfe (1983) to explain their MgII survey for 21 cm absorbers. They proposed a two-phase model where the 21 cm absorption is produced in galaxy disks, and the metal-line components that do not produce 21 cm absorption are produced in galactic halos. However, this multi-component/cloud model could be valid in any gas-rich galaxy, as is evidenced by DLA galaxy imaging studies (Le Brun et al. 1997; Rao & Turnshek 1998; Turnshek et al. 2001; Rao et al. 2003; Turnshek et al. 2004). The disk models of Prochaska & Wolfe (1997) and the Haehnelt et al. (1998) models of infalling and merging clouds could reproduce these observations equally well. In other words, DLAs arise in pockets of cold gas embedded within warm diffuse gas or gas clouds in any bound system.

Twenty one cm observations of low-redshift DLAs also reveal some cloud structure. For example, the $z = 0.313$ system towards PKS 1127–145 shows 5 components and the $z = 0.394$ system towards B0248+430 is resolved into 3 components (Lane 2000; Lane & Briggs 2001; Kanekar & Chengalur 2001). Since the MgII line for these systems has not been observed at a resolution as high as the 21 cm observations, a one-to-one correspondence between the metal-line and 21 cm clouds cannot be drawn. In other instances, both warm and cold gas have been detected in a 21 cm DLA; Lane et al. (2000) find that two-thirds of the column density in the $z = 0.0912$ DLA towards B0738+313 is contained in warm phase gas, and the rest is contained in two narrow components. The $z = 0.2212$ absorber towards the same quasar was also found to exhibit similar characteristics (Kanekar et al. 2001). In each of these cases, the line of sight probably intersects two cold clouds in addition to warm diffuse gas spread over a wider range of velocities that can be detected only in 21 cm observations of very high sensitivity. There are also several instances of DLAs not being detected at 21 cm (Kanekar & Chengalur 2003). High spin temperatures ($T_s > 1000$ K) corresponding to warm diffuse gas and/or covering factors less than unity towards extended quasar radio components have been suggested as possible explanations (Kanekar & Chengalur 2003; Curran et al. 2005).

Clearly, a wide variety of cloud properties and their combinations are responsible for the observed properties of MgII, DLA, and 21 cm absorption lines. Observations in the 21 cm line have the added complication that the background radio and optical sources may sample different sightlines, thus making interpretation difficult. DLA observations, on the other hand, do not suffer from this effect. Large simulations of galaxy sightlines with varying cloud properties that reproduce the metal-line, DLA correlations shown in Figures 2–7 should be the next step towards improving our understanding of these absorption line systems. The simulations should not only reproduce the frequency of occurrence of DLAs in MgII systems, but also the number density evolution of MgII systems and DLAs.

3.3. The redshift number density of DLAs, n_{DLA}

The redshift number density of DLAs, n_{DLA} , sometimes written as dn/dz , can be determined using the equation

$$n_{DLA}(z) = f(z) n_{MgII}(z), \quad (3.1)$$

where $f(z)$ is the fraction of DLAs in a MgII sample as a function of redshift and $n_{MgII}(z)$ is the redshift number density of MgII systems. With the systems detected in SDSS EDR quasar spectra, Nestor (2004) derived

$$dn/dz = N^* (1+z)^\alpha e^{-\frac{W_0}{W^*}(1+z)^{-\beta}}, \quad (3.2)$$

where we have retained his notation and $W \equiv W_0^{\lambda 2796}$ (see also NTR05). N^* , W^* , α , and β are constants. This expression is an integral over all $W_0^{\lambda 2796}$ greater than W_0 . Since our MgII sample was assembled under various selection criteria that were modified based on our initial results (RT00), $n_{DLA}(z)$ had to be evaluated carefully. Again, we refer the reader to RTN05 for details on how $n_{DLA}(z)$ was determined.

Figure 8 shows the results for $n_{DLA}(z)$ at low redshift split into two redshift bins (solid squares). We find 18 DLAs in 104 MgII systems in the redshift interval $0.11 < z \leq 0.9$ with $n_{DLA}(z = 0.609) = 0.079 \pm 0.019$ and 23 DLAs in 94 MgII systems in the redshift interval $0.9 < z \leq 1.65$ with $n_{DLA}(z = 1.219) = 0.120 \pm 0.025$. The points are plotted at the mean redshift of the MgII samples. The high-redshift data points are from Prochaska & Herbert-Fort (2004) and the $z = 0$ point was estimated by Zwaan (in preparation) from a WSRT survey of HI in the local universe. The solid curve in Figure 8a is a no-evolution curve in the standard Λ CDM cosmology, that we refer to as the “737” cosmology, where $(h, \Omega_M, \Omega_\Lambda) = (0.7, 0.3, 0.7)$. This curve, which has been normalized at the $z = 0$ data point, shows that the comoving cross-section for absorption declined rapidly by a factor of ≈ 2 until $z \approx 2$ and has remained constant since then. This behavior might be a consequence of what has been observed in other studies of galaxy evolution, namely, that today’s galaxies were in place by $z \approx 1$ and are a consequence of rapid merger and/or collapse events that occurred prior to this epoch.

It has been customary in quasar absorption line studies to plot the logarithm of the redshift number density in order to illustrate its power law dependence with redshift, i.e., $n(z) = n_0(1+z)^\gamma$. In $\Lambda = 0$ cosmologies, the exponent is a measure of the evolution in this quantity. For example, $\gamma = 1$ for $q_0 = 0$ or $\gamma = 0.5$ for $q_0 = 0.5$ imply no intrinsic evolution of the absorbers, and any significant departure from these values for γ is evidence for evolution in the comoving number density of absorbers. We plot $\log n_{DLA}(z)$ as a function of $\log(1+z)$ in Figure 8b. The straight line is the power law fit to the data points with slope $\gamma = 1.27 \pm 0.11$, and the curve is the same no-evolution function shown in the left panel. Thus, in the past the observations would have been interpreted as being consistent with the DLA absorbers undergoing no intrinsic evolution in a $q_0 = 0$ universe, and marginally consistent with evolution in a $q_0 = 0.5$ universe. With the now widely accepted concordance cosmology, the interpretation has changed quite dramatically; as noted above, the nature of the evolution is redshift dependent.

The possibility of a dust bias in DLA statistics at low redshift was addressed by Ellison et al. (2004) using the same CORALS survey that Ellison et al. (2001) used to show that the effect of dust at $z \approx 2$ was minor. They determined the MgII dn/dz for redshifts $0.6 < z < 1.7$, and found excellent agreement with the results of NTR05 who used the SDSS-EDR quasar sample. Based on the RT00 strong MgII-FeII selection for DLAs, they concluded that dust bias was not important for DLAs at low redshift either.

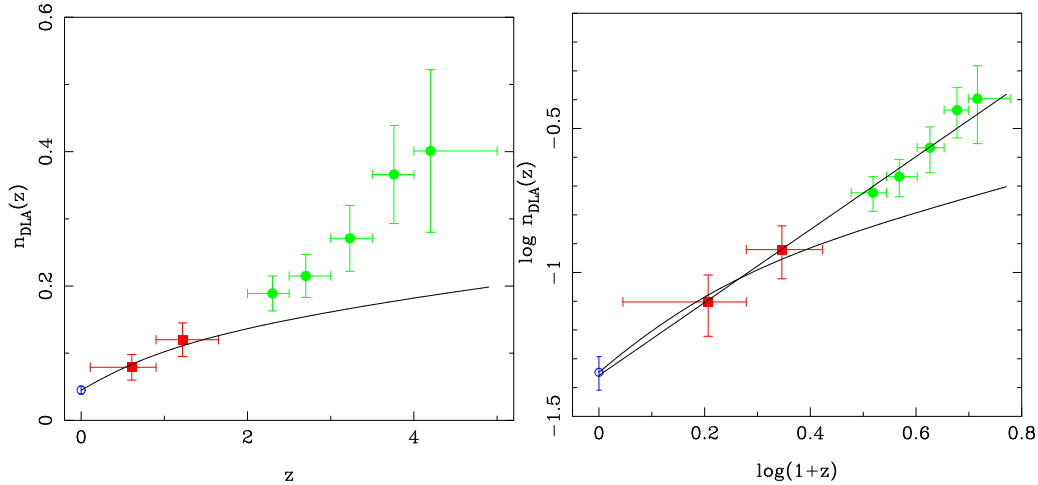


Figure 8. *Left, a:* Plot of $n_{DLA}(z)$ versus redshift. The new low-redshift data points from RTN05 are shown as filled squares. The high-redshift points (filled circles) are from Prochaska & Herbert-Fort (2004) and the $z = 0$ data point is from an analysis of local HI (Zwaan, in preparation). The solid line is a no-evolution curve in the “737” cosmology with $(h, \Omega_M, \Omega_\Lambda) = (0.7, 0.3, 0.7)$ normalized at $z = 0$. The comoving cross-section for absorption declined rapidly by a factor of ≈ 2 until $z \approx 2$ and has remained constant since then. *Right, b:* Plot of $\log n_{DLA}(z)$ as a function of $\log(1+z)$. The straight line is the power law fit to the data points with slope $\gamma = 1.27 \pm 0.11$, and the curve is the no-evolution function shown in Figure 8a.

3.4. The cosmological mass density Ω_{DLA}

We can determine Ω_{DLA} from the DLA column densities and $n_{DLA}(z)$ via the expression

$$\Omega_{DLA}(z) = \frac{\mu m_H H_0}{c \rho_c} n_{DLA}(z) \langle N(HI) \rangle \frac{E(z)}{(1+z)^2}, \quad (3.3)$$

where

$$E(z) = (\Omega_M(1+z)^3 + (1 - \Omega_M - \Omega_\Lambda)(1+z)^2 + \Omega_\Lambda)^{1/2}. \quad (3.4)$$

Again, the “737” cosmology has been used in the calculation of Ω_{DLA} . Also, $\mu = 1.3$ corrects for a neutral gas composition of 75% H and 25% He by mass, m_H is the mass of the hydrogen atom, ρ_c is the critical mass density of the universe, and $\langle N(HI) \rangle$ is the mean HI column density of DLAs in each redshift bin.

In contrast to the redshift number density evolution shown in Figure 8, we find that Ω_{DLA} has remained constant from $z = 5$ to $z = 0.5$ to within the uncertainties. Figure 9 shows the new results as solid squares. Specifically, for the redshift range $0.11 < z \leq 0.90$, we find $\Omega_{DLA}(z = 0.609) = (9.7 \pm 3.6) \times 10^{-4}$ and for the range $0.90 < z < 1.65$ we get $\Omega_{DLA}(z = 1.219) = (9.4 \pm 2.8) \times 10^{-4}$. The uncertainties have been reduced considerably in comparison to our results in RT00. The reasons for this are two fold. First, the uncertainty in n_{MgII} has been significantly reduced due to the fact that the MgII sample size was increased 10-fold. Second, the number of DLAs in each bin has increased by more than a factor of 3. Thus, the uncertainties in the low- and high-redshift data points are now comparable. Note that the statistics of the high-redshift data are also improved due to the inclusion of an SDSS DLA sample (Prochaska & Herbert-Fort 2004). Nevertheless, our basic conclusion from RT00 has remained unchanged, namely, that the cosmological mass density of neutral gas remains roughly constant from $z \approx 5$ to $z \approx 0.5$.

The drop in redshift number density from $z = 5$ to $z = 2$ along with a constant mass density in this range indicates that while the product of galaxy cross-section and co-

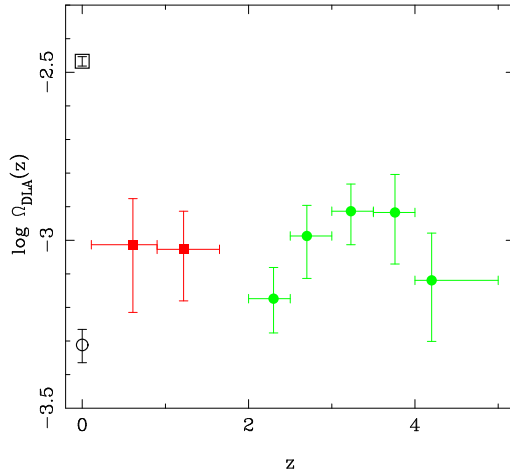


Figure 9. Cosmological mass density of neutral gas, Ω_{DLA} , as a function of redshift. The filled squares are the new low-redshift data points from RTN05. The high-redshift points (filled circles) are from Prochaska & Herbert-Fort (2004) and the open circle at $z = 0$ is from Zwaan et al. (2005). The open square at $z = 0$ is the mass density in stars estimated by Panter et al. (2004) from SDSS data. While the statistics have improved considerably, our basic conclusion from RT00 has remained unchanged, namely, that the cosmological mass density of neutral gas has remained constant from $z \approx 5$ to $z \approx 0.5$.

moving number density is declining, the mean column density per absorber is increasing. This is, again, consistent with the assembly of higher density clouds as galaxy formation proceeds.

On the other hand, a constant cross-section from $z \approx 1$ to $z = 0$ along with a drop in mass density from $z \approx 0.5$ to $z = 0$ is indicative of star formation that depletes the highest column density gas while keeping the absorption cross-section constant. This would in turn require that the column density distribution of DLAs change such that the ratio of high to low column densities decreases from low-redshift to $z = 0$. As we will see in the next section, the column density distribution does show some evidence for this.

3.5. The column density distribution $f(N)$

Figure 10 shows the normalized cumulative column density distribution (CDD) for the three redshift regimes. The dotted curve is the $z = 0$ distribution derived by Ryan-Weber et al. (2003, 2005) from HIPASS data. The red (thick, solid) curve is derived from the 41 DLAs at low redshift (RTN05) and the green (thin, solid) curve is from the “total” sample of Prochaska & Herbert-Fort (2004). The change in the three CDDs with redshift is exactly what is expected based on the n_{DLA} and Ω_{DLA} results. Namely, that the low-redshift CDD shows a higher incidence of high column density systems than at high redshift presumably due to the assembly of gas as galaxy formation proceeds, followed by a decrease in the fraction of high column density systems to $z = 0$, presumably due to the depletion of gas during star formation. Thus, at least qualitatively, the evolutionary behavior of n_{DLA} , Ω_{DLA} , and the CDD are entirely consistent with one another. A KS test shows that there is a 25% probability that the high- and low-redshift curves are drawn from the same population; this is significantly higher than what we observed in RT00, where the two samples had only a 2.8% probability of being drawn from the same population. However, the general trend that the low-redshift sample has a higher fraction of high column density system still remains.

Figure 11 is a plot of the log of the absolute CDD function, $\log f(N)$, as a function of

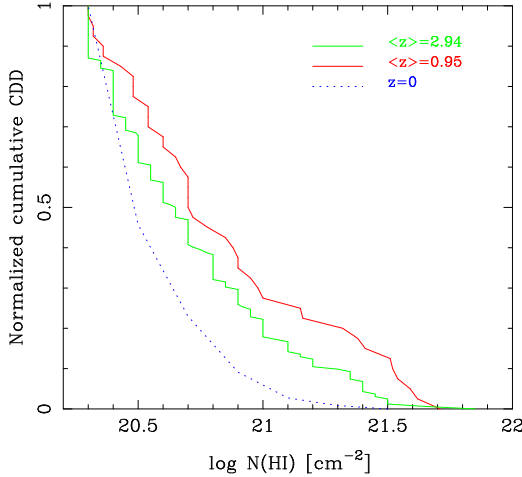


Figure 10. The normalized cumulative CDD of DLAs for three redshift regimes. The red, thick solid line includes the 41 low-redshift DLAs at $\langle z \rangle = 0.95$ (RTN05). The green, thin solid line includes 163 high-redshift DLAs at $\langle z \rangle = 2.94$ (Prochaska & Herbert-Fort 2004), and the blue, dotted curve is the $z = 0$ estimate from Ryan-Weber et al. (2003, 2005).

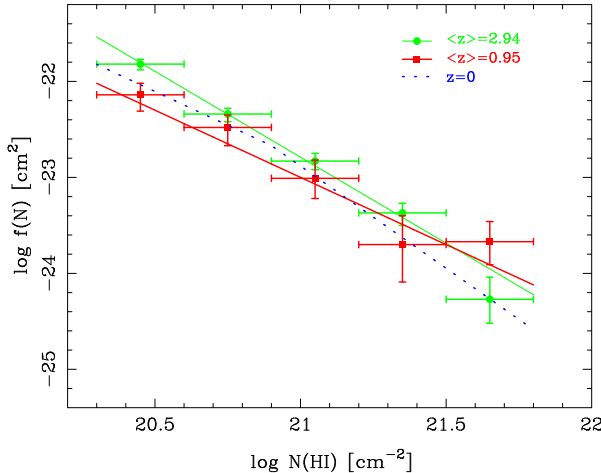


Figure 11. Absolute CDD function for the three redshift regimes. The red, thick solid line is a least squares fit to the low-redshift data points (RTN05) and has slope $\beta = 1.4$; the green, thin solid line is a least squares fit to the high-redshift data points (Prochaska & Herbert-Fort 2004) with $\beta = 1.8$. The dotted line is the CDD with $\beta = 1.4$ for $\log N(HI) < 20.9$ and $\beta = 2.1$ for $\log N(HI) \geq 20.9$ (Ryan-Weber et al. 2003, 2005).

$\log N(HI)$ for the three redshift regimes. The turnover with redshift is most apparent in the lowest and highest column density bins. We derive $\beta = 1.4 \pm 0.2$ and $\beta = 1.8 \pm 0.1$ at low and high redshift respectively, where the CDD is expressed as $f(N) = BN^{-\beta}$. At $z = 0$, Ryan-Weber et al. (2003) derive $\beta = 1.4 \pm 0.2$ for $\log N(HI) < 20.9$ and $\beta = 2.1 \pm 0.9$ for $\log N(HI) \geq 20.9$. The general form of the absolute CDD does not vary considerably with redshift, which in turn explains the roughly constant value of Ω_{DLA} . The differences in the $f(N)$ distributions are subtle, implying that the gas content in DLAs is not changing drastically. This is strong evidence that DLAs do not have high SFRs and are, therefore, a different population of objects than those responsible for

much of the observed luminosity in the high redshift universe. On the other hand, a non-evolving DLA population might be observed if the gas that is used up in star formation is replenished from the inter-galactic medium at a comparable rate. This possibility seems rather contrived, and requires more proof than the current observational evidence can provide. In the next section, we discuss further evidence that suggests that DLAs and Lyman break galaxies (LBGs) are mutually exclusive galaxy populations.

4. The Nature of DLAs

With the identification of DLAs in quasar spectra, follow-up work involving the study of DLA galaxies, their environments, DLA gas metallicities, kinematics, temperatures, and ionization conditions, and numerical and semi-analytic modelling has kept many astronomers busy for decades. A keyword search for “damped Ly” in NASA’s abstract database returns nearly 1000 results, too many to reference here. Despite this, a consensus on the nature of these objects is still lacking. One of the primary reasons for this is that the selection effects inherent in the observations are still being sorted out. Many of these issues were raised at this conference, and we address some of them here. See also Turnshek et al. (2005, these proceedings) for further discussion on DLA selection effects.

The conclusion that DLA surveys identify the bulk of the neutral gas in the universe is based on three results or assumptions. First, integration of the CDD shows that a relatively small fraction of the neutral gas is contributed by Lyman limit and sub-DLA absorption systems with $3 \times 10^{17} < N(HI) < 2 \times 10^{20} \text{ cm}^{-2}$, at least for $z < 3.5$ (Péroux et al. 2003), and perhaps at all redshifts (Prochaska & Herbert-Fort 2004). Second, as discussed earlier, dusty regions do not cause DLA surveys to miss a large fraction of the neutral gas (Ellison et al. 2001, 2004). Third, the biases introduced by gas cross section selection are small. The important points to emphasize here are that the interception (or discovery) probability is the product of gas cross section times comoving absorber number density, and no DLAs with $N(HI) > 8 \times 10^{21} \text{ cm}^{-2}$ have been discovered. Thus, the third assumption requires that rare systems with relatively low gas cross section and very high HI column density are either absent or have not been missed to the extent that the neutral gas mass density will be significantly underestimated by quasar absorption line surveys. This third assumption might have to be reevaluated in order to explain the discrepancy between the star formation history (SFH) of DLAs as inferred from their HI column densities and that determined from galaxies that trace the optical luminosity function. We explored this connection in Hopkins, Rao, & Turnshek (2005) and summarize it here.

We can use the global Schmidt law relating gas surface density and SFR to infer the star forming properties of the DLAs. Assuming that the Schmidt law, quantified by Kennicutt (1998), is valid at the DLA redshifts we can convert DLA column densities into gas surface densities and estimate their SFR. In Hopkins et al. (2005) we show that the SFR density of DLAs relates to $n_{DLA}(z)$ and $\Omega_{DLA}(z)$ as follows:

$$\dot{\rho}_* = 4.0 \times 10^{-15} \left(\frac{dX/dz}{n_{DLA}} \right)^{0.4} \left(\frac{\Omega_{DLA}}{\mu} \rho_c \right)^{1.4} \quad (4.1)$$

where $\dot{\rho}_*$ is the SFR density in units of $\text{M}_\odot \text{ yr}^{-1} \text{ Mpc}^{-3}$ and dX/dz is the absorption distance which equals $(c/H_0)(1+z)^2/E(z)$. $E(z)$, μ , and ρ_c are as defined in §3.4. Figure 12 shows the SFR density of DLAs estimated using equation 4.1 and the values of $n_{DLA}(z)$ and $\Omega_{DLA}(z)$ plotted in Figures 8 and 9. The hatched region encompasses the majority of SFR estimates in the literature (Hopkins 2004) and the solid curve is a fit to these data. The crosses are estimates of the SFR in DLAs using the CII* absorption

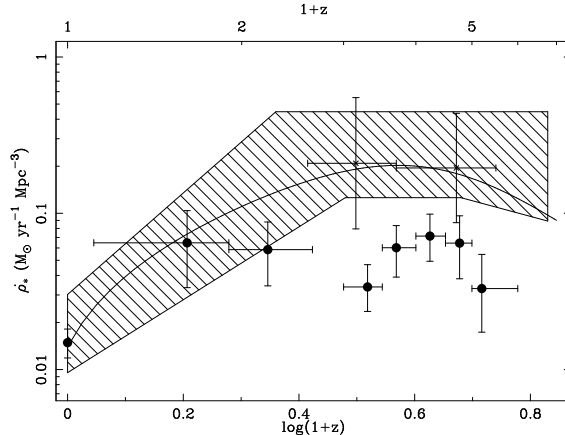


Figure 12. SFR density of DLAs (filled circles) as a function of redshift from Hopkins, Rao, & Turnshek (2005). Crosses are estimates from Wolfe et al. (2003) using the CII* method (but see footnote). The hatched region encompasses the majority of SFR estimates in the literature (Hopkins 2004) and the solid curve is a fit to these data.

line technique of Wolfe et al. (2003). The CII* results are consistent with the fitted curve derived from the SFH of luminous galaxies, and have been interpreted as evidence that the DLA population is the same as the LBGs†. However, the few high-redshift DLAs for which host galaxies have been identified yield SFRs that are at the very faint end of values determined for LBGs (e.g., Weatherley et al. 2005, Møller et al. 2002). Recent results from semi-analytic models and numerical simulations by Okoshi & Nagashima (2005) and Nagamine et al. (2004) indicate that the average masses of DLA galaxies are likely to be low, around $10^9 M_\odot$, which is consistent with low integrated levels of SFR. Okoshi & Nagashima (2005) find a broad range of SFRs from 10^{-6} to $100 M_\odot \text{ yr}^{-1}$, with a mean value of $0.01 M_\odot \text{ yr}^{-1}$ for DLAs at redshifts $z < 1$, and conclude that DLAs are typically dwarf systems with low SFRs. Therefore, it is entirely possible that the high redshift observations of Weatherley et al. (2005), and Møller et al. (2002) are sampling the brightest end of DLA galaxy properties. Lanzetta et al. (2002) have also shown, through similar HI surface density and SFR arguments that LBGs have SFR surface densities that are up to 3 orders of magnitude higher than that of the DLAs. In fact, their SFR densities do not overlap for the observed DLA redshift range $1.65 < z < 5$ (see Lanzetta et al. figure 3b). This implies that the high SFR surface density objects have very high column density neutral plus molecular gas (10^{22} to 10^{25} cm^{-2}). These are comparable to the surface gas and SFR densities seen in local starburst nuclei (Kennicutt 1998). Observations of local star forming galaxies have shown that $N(\text{HI})$ is always $\gtrsim 10^{-2} N(H_2)$ in the high SFR regions (e.g., Wong & Blitz 2002), and therefore, could lie above the currently observed DLA regime. If these systems have very small interception cross sections, they may be missed in surveys for DLAs. For example, an absorber with a size of about 100 pc, comparable to giant molecular clouds (GMCs) which are the sites of star formation, has a cross section that is $\approx 10^4$ times smaller than known DLAs, which typically have effective radii of ≈ 10 kpc (Monier et al. 2005). Assuming that there are on the order of 10 GMCs per galaxy, the total cross section per unit volume, i.e., interception probability, for these very high column density gas systems would be on the order

† Using more recent UV background radiation estimates, Wolfe (2005, these proceedings) finds lower CII* estimates of DLA SFR density which are now in agreement with the Hopkins et al. result.

of 10^3 times smaller. This means that 10^3 DLAs need to be detected in order to find one very high column density system. With the SDSS, we are getting close, but are not quite there yet. A one in a thousand system with $N(HI + H_2) = 10^{24} \text{ cm}^{-2}$ would increase the SFR density of DLAs by more than a factor of 2, and bring the DLA SFR density into agreement with the luminous SFR density. Searches for molecular gas in DLAs have resulted in only a handful of detections. Moreover, the molecular gas fraction in the few DLAs with H_2 detections is very small (e.g. Ledoux et al. 2003), and is consistent with the idea that the known sample of DLAs does not trace the majority of the star forming gas in the universe.

A similar conclusion is reached when considering the low metallicities of DLAs. Figure 13a shows the most recent compilation of DLA metallicities from Rao et al. (2005b). Pettini and collaborators were the first to make metallicity measurements of a large number of DLAs; the early data indicated that DLA metallicities do not evolve from redshifts $z \approx 3.5$ to $z \approx 0.5$ (Pettini et al. 1999 and references therein). With a much larger sample, Prochaska et al. (2003) and Rao et al. (2005b), the latter with more measurements at $z < 1.65$, showed that DLA metallicities do show evidence for evolution. In Figure 13b, we show the metal mass density as a function of redshift. The DLA metallicity data from Rao et al. (2005b) are converted to metal mass by assuming $\log \Omega_{DLA} = -3$ and a solar metal mass fraction of $Z_\odot = 0.02$. The metal mass density in stars, shown as the hatched region in Figure 13b, can be derived from the SFR, since the SFR is related to the metal production rate (e.g., Madau et al. 1996). Stellar population synthesis results indicate that $\dot{\rho}_* = 63.7\dot{\rho}_Z$ (Bruzual & Charlot 2003, Conti et al. 2003). The $z = 0$ and $z = 2.5$ results of Dunne et al. (2003) are also shown. Dunne et al. used the dusty, high SFR, submillimeter galaxy population at $z = 2.5$ to derive their result, which is reasonably consistent with the evolution of ρ_Z from the SFH. They concluded that high redshift DLAs are not the same population as these star forming galaxies, which contain the majority of the metals at this epoch. The DLAs have about two orders of magnitude less mass in metals than star forming galaxies. The combination of low metallicity and low gas mass density naturally leads to a space density of metals that is significantly lower than in the luminous galaxy population. This “missing metals” problem cannot be solved simply by invoking spheroids, dwarfs, low surface brightness galaxies, or gas at large galactocentric distance. Instead, this problem may in fact be the result of missing a substantial fraction of the metal-enriched gas in DLA surveys, for example in the GMCs mentioned above, due to their very small interception probability. That molecules are detected in DLAs with higher than average metallicities is consistent with this idea (Ledoux et al. 2003). Thus, the SFH and missing metals problem can both be attributed to this same selection effect. All of this holds true at high redshift. We note, however, that the SFR in DLAs and luminous objects at $z < 1$ are comparable, but their metal mass densities are not. This can be explained by noting that by $z \approx 1$, the SFR in luminous, high SFR, galaxies begins to decline, i.e., the luminosity density of the universe fades, leaving behind the low SFR DLA galaxies as the main contributor to the volume averaged SFR. The metal mass density, on the other hand, has been building up in the high SFR galaxies at high redshift, and continues to remain high. In fact, ρ_Z plateaus at $z \lesssim 1$ because the DLAs have low SFRs and do not increase the metal mass density significantly.

However, the possibility that these very high column density gas systems are being missed by DLA surveys may not only be due to their small gas cross sections, but also because they are likely to be very dusty. Ledoux et al. (2003) find that the DLAs in which H_2 is detected have among the highest metallicities and the highest depletion factors, hinting at the possibility of much higher depletions in much higher column density molecular gas clouds. These are not found in the radio loud quasar surveys for DLAs

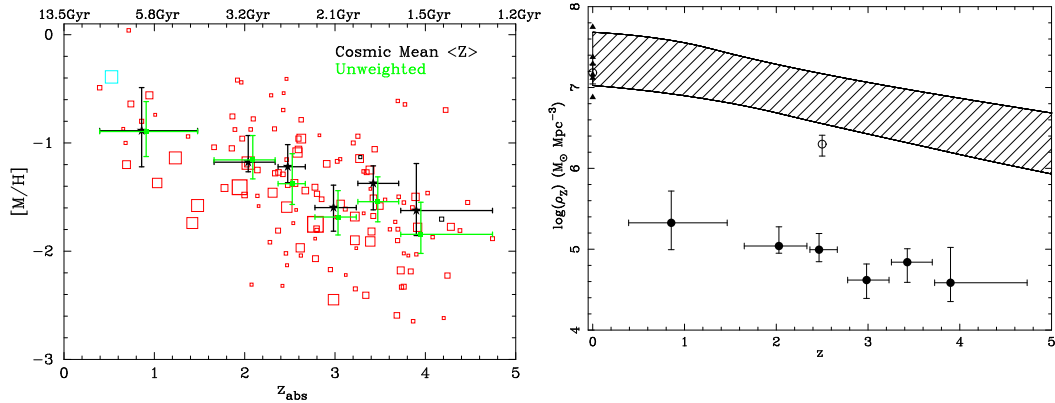


Figure 13. *Left, a:* Metallicity vs. redshift for DLAs plotted as open squares where the area of each square is proportional to $N(HI)$ (Rao et al. 2005b, Prochaska et al. 2003). The cosmic mean metallicities weighted by $N(HI)$, $\langle Z \rangle$, are filled stars and the unweighted mean metallicities are filled circles. The best fit linear slope is $m = -0.26 \pm 0.06$, indicating increasing metallicity with time. *Right, b:* Metal mass density as a function of redshift from Hopkins et al. (2005). Solid circles are DLA metallicities from Figure 13a converted to mass density, and the hatched region is derived from the SFH corresponding to the hatched region in Figure 12. Triangles at $z = 0$ are from Calura & Matteucci (2004); open circles are from Dunne et al. (2003).

because these surveys also suffer from the small cross section selection effect. Not enough radio loud quasars have yet been surveyed to find the putative one in a thousand very high column density system.

Gravitational lensing has the opposite effect on DLA surveys. Magnification by DLA galaxies could brighten background quasars, and preferentially include them in magnitude-limited samples. Le Brun et al. (2000), with HST imaging observations, showed no evidence for multiple images of background quasars and concluded that the quasars were magnified by at most 0.3 magnitudes. In addition, Ellison et al. (2004) and Péroux et al. (2004) using statistical tests on low redshift MgII and DLA samples, showed that lensing bias is a minor effect. More recently, using the SDSS MgII survey results of Nestor (2004), Ménard et al. (2005) show that quasars behind strong MgII absorbers, of which DLAs are a subset, show little magnification bias, and that its effect on Ω_{DLA} at low redshift is negligible (see also Ménard 2005). It is also unlikely that the lowest redshift points that we derived from our HST-UV data (Figure 9) are affected by lensing bias. This is because the DLAs with the highest HI column densities at $z \approx 0.5$ arise in dwarf galaxies (Rao et al. 2003), and consequently, do not have the mass required to produce significant magnification.

5. Summary

Since the discovery of DLAs in the early 1970s, a considerable amount of effort has been put into deciphering the properties of neutral gas in the universe. The observational techniques that have to be used to trace the neutral gas separate the Ly α universe into three redshift regimes: the optical/IR at $z > 1.65$, the UV at $0 < z < 1.65$, and the radio (21 cm) at $z = 0$. The current status of DLA surveys in these three redshift regimes was reviewed; while the $z = 0$ and $z > 1.65$ regimes have been more than adequately serviced by nearly all-sky surveys, the UV regime could do with an order of magnitude more DLAs. We also put forward a change in the paradigm that DLAs trace the bulk of the neutral gas in the universe. Selection effects that preclude us from observing the highest

column density gas might be affecting our interpretation of what DLA statistics really mean. Evidence for this comes from a comparison of DLA and luminous mass densities, SFRs, and metal mass densities as a function of redshift. See Turnshek et al. (2005, these proceedings) for more discussion on DLA selection effects.

Acknowledgements

I thank the organizing committee and Shanghai Astronomical Observatory for hosting a lively and productive conference. I would like to acknowledge Dave Turnshek, Art Wolfe, Chris Churchill, Andrew Hopkins, Brice Ménard, Jason Prochaska, and Martin Zwaan for helpful discussions. This work was funded by grants from NASA-STScl, NASA-LTSA, and NSF. HST-UV spectroscopy made the $N(HI)$ determinations possible. We thank members of the SDSS collaboration who made the SDSS project a success. Funding for creation and distribution of the SDSS Archive has been provided by the Alfred P. Sloan Foundation, Participating Institutions, NASA, NSF, DOE, the Japanese Monbukagakusho, and the Max Planck Society. The SDSS Web site is www.sdss.org. The SDSS is managed by the Astrophysical Research Consortium for the Participating Institutions: University of Chicago, Fermilab, Institute for Advanced Study, the Japan Participation Group, Johns Hopkins University, Los Alamos National Laboratory, the Max-Planck-Institute for Astronomy (MPIA), the Max-Planck-Institute for Astrophysics (MPA), New Mexico State University, University of Pittsburgh, Princeton University, the United States Naval Observatory, and University of Washington.

References

Bahcall, J. N. & Spitzer, L. 1969, ApJ, 156, L63
 Beaver, E. A., Burbidge, E. M., McIlwain, C. E., Epps, H. W., & Strittmatter, P. A. 1972, ApJ, 178, 95
 Briggs, F. H. 1988, in QSO Absorption Lines: Probing the Universe, ed. S. C. Blades, D. A. Turnshek, & Norman, C. A. (Cambridge: Cambridge Univ. Press), 275
 Briggs, F. H. 1999, in ASP Conf. Ser. 156, Highly Redshifted 21 cm Lines, ed. C. L. Carilli, S. J. E. Radford, Menten, K. M., & Langston, G. I., 16
 Briggs, F. H., Wolfe, A. M., Krumm, N., & Salpeter, E. E. 1980, ApJ, 238, 510
 Briggs, F. H. & Wolfe, A. M. 1983, ApJ, 268, 76
 Brown, R. L. & Roberts, M. S. 1973, ApJ, 184, L7
 Bruzual, G. & Charlot, S. 2003, MNRAS, 344, 1000
 Carswell, R. F., Hilliard, R. L., Strittmatter, P. A., Taylor, D. J., & Weymann, R. J. 1975, ApJ, 196, 351
 Caulet, A. 1989, ApJ, 340, 90
 Calura, F. & Matteucci, F. 2004, MNRAS, 350, 351
 Churchill, C. W. 2001, ApJ, 560, 92
 Churchill, C. W., Vogt, S. S., & Charlton, J. C. 2003, AJ, 125, 98
 Cohen, R. D., Barlow, T. A., Beaver, E. A., Junkkarinen, V. T., Lyons, R. W., & Smith, H. E. 1994, ApJ, 421, 453
 Conti, A., et al. 2003, AJ, 126, 2330
 Curran, S. J., Murphy, M. T., Pihlström, Y. M., Webb, J. K., & Purcell, C. R. 2005, MNRAS, 356, 1509
 Dunne, L., Eales, S. A., & Edmunds, M. G. 2003, MNRAS, 341, 589
 Ellison, S. L., Yan, L., Hook, I. M., Pettini, M., Wall, J., & Shaver, P. 2001, A&A, 379, 393
 Ellison, S. L., Churchill, C. W., Rix, S. A., & Pettini, M. 2004, ApJ, 615, 118
 Fall, S. M. & Pei, Y. 1989, ApJ, 337, 7
 Fall, S. M. & Pei, Y. 1993, ApJ, 402, 479
 Haehnelt, M. G., Steinmetz, M., & Rauch, M. 1998, ApJ, 495, 647
 Hopkins, A. 2004, ApJ, 615, 209

Hopkins, A. M., Rao, S. M., & Turnshek, D. A. 2005, ApJ, submitted

Jannuzzi, B. T. et al. 1998, ApJS, 118, 1

Kanekar, N. & Chengalur, J. 2001, MNRAS, 325, 631

Kanekar, N. & Chengalur, J. 2003, A&A, 399, 857

Kanekar, N., Ghosh, T., & Chengalur, J. N. 2001, A&A, 373, 394

Keeney, B. A., Momjian, E., Stocke, J. T., Carrilli, C. L., & Tumlinson, J. 2005, ApJ, 622, 267

Kennicutt, R. C. 1998, ApJ, 498, 541

Kinney, A. L., Bohlin, R. C., Blades, J. C., & York, D. G. 1991, ApJS, 75, 645

Lane, W. 2000, Ph.D. Thesis, Univ. Groningen

Lane, W. M. & Briggs, F. H. 2001, in ASP Conf. Ser. 254, Extragalactic Gas at Low Redshift, ed. J. Mulchaey & J. Stocke (San Francisco: ASP), 189

Lane, W. M., Briggs, F. H., Smette, A. 2000, ApJ, 532, 146

Lanzetta, K. M., Wolfe, A. M., Turnshek, D. A., Lu, L., McMahon, R. G., & Hazard, C. 1991, ApJS, 77, 1

Lanzetta, K. M., Turnshek, D. A., & Sandoval, J. 1993, ApJS, 84, 109

Lanzetta, K. M., Turnshek, D. A., & Wolfe, A. M. 1987, ApJ, 322, 739

Lanzetta, K. M., Wolfe, A. M., & Turnshek, D. A. 1995, ApJ, 440, 435

Lanzetta, K. M., Yahata, N., Pascarelle, S., Chen, H.-W., & Fernandez-Soto, A. 2002, ApJ, 570, 492

Le Brun, V., Bergeron, J., Boissé, P., & Deharveng, J. M. 1997, A&A, 321, 733

Le Brun, V., Smette, A., Surdej, J., & Claeskens, J.-F. 2000, A&A, 363, 837

Ledoux, C., Petitjean, P., & Srianand, R. 2003, MNRAS, 346, 209

Lowrance, J. L., Morton, D. C., Zucchini, P., Oke, J. B., & Schmidt, M. 1971, BAAS, 3, 238

Lowrance, J. L., Morton, D. C., Zucchini, P., Oke, J. B., & Schmidt, M. 1972, ApJ, 171, 233

Lynds, R. 1971, ApJ, 164, L73

Madau, P., Ferguson, H. C., Dickinson, M. E., Giavalisco, M., Steidel, C. C., Fruchter, A. 1996, MNRAS, 283, 1388

Ménard, B. 2005, ApJ, in press (astro-ph/040827)

Ménard, B., et al. 2005, in preparation

Minchin, R. F., et al. 2003, MNRAS, 346, 787

Minchin, R. F., et al. 2004, MNRAS, 355, 1303

Møller, P., Warren, S. J., Fall, S. M., Fynbo, J. U., & Jakobsen, P. 2002, ApJ, 574, 51

Monier, E. M., Turnshek, D. A., & Rao, S. M. 2005, in preparation

Nagamine, K., Springel, V., & Hernquist, L. 2004, MNRAS, 348, 435

Nestor, D. B 2004, Ph.D. Thesis, Univ. Pittsburgh

Nestor, D. B., Turnshek, D. A., & Rao, S. 2005, ApJ, in press, astro-ph/0410493 (NTR05)

Okoshi, K. & Nagashima, M. 2005, ApJ, 623, 99

Panter, B., Heavens, A. F., & Jimenez, R. 2004, MNRAS, 355, 764

Pei, Y., Fall, S. M., & Hauser, M. G. 1999, ApJ, 522, 604

Péroux, C., Storrie-Lombardi, L. J., McMahon, R. G., Irwin, M. J., & Hook, I. 2001, AJ, 121, 1799

Péroux, C., McMahon, R. G., Storrie-Lombardi, L. J., & Irwin, M. J. 2003, MNRAS, 346, 1103

Péroux, C., Deharveng J.-M., Le Brun, V., & Cristiani, S. 2004, MNRAS, 352, 1291

Pettini, M., Ellison, S. L., Steidel, C. C., & Bowen, D. 1999, ApJ, 510, 576

Prochaska, J. X. & Wolfe, A. M. 1997, ApJ, 487, 73

Prochaska, J. X., Gawiser, E., Wolfe, A. M., Castro, S., & Djorgovski, S. G. 2003, ApJ, 595, L9

Prochaska, J. X. & Herbert-Fort, S. 2004, PASP, 116, 622

Prochaska, J. X., et al. 2005, these proceedings

Rao, S. M. 1994, Ph.D. Thesis, Univ. Pittsburgh

Rao, S. M. & Briggs, F. H. 1993, ApJ, 419, 515

Rao, S. M., Turnshek, D. A., & Briggs, F. H. 1995, ApJ, 449, 488

Rao, S. M. & Turnshek, D. A. 1998, ApJ, 500, L115

Rao, S. M. & Turnshek, D. A. 2000, ApJS, 130, 1 (RT00)

Rao, S. M., Nestor, D. B., Turnshek, D. A., Lane, W. M., Monier, E. M., & Bergeron, J. 2003, ApJ, 595, 94

Rao, S. M. & Turnshek, D. A. 2000, *ApJS*, 130, 1 (RT00)

Rao, S. M., Turnshek, D. A., & Nestor, D. B. 2005a, *ApJ*, submitted (RTN05)

Rao, S. M., Prochaska, J. X., Howk, J. C., & Wolfe, A. M. 2005b, *AJ*, 129, 9

Rosenberg, J., & Schneider, S. E. 2000, *ApJS*, 130, 177

Ryan-Weber, E. V., Webster, R. L., Staveley-Smith, L. 2003, *MNRAS*, 343, 1195

Ryan-Weber, E. V., Webster, R. L., Staveley-Smith, L. 2005, *MNRAS*, 356, 1600

Sargent, W. L. W., Young, P. J., Boksenberg, A., & Tytler, D. 1980, *ApJS*, 42, 41

Sargent, W. L. W., Steidel, C. C., & Boksenberg, A. 1988, *ApJ*, 334, 22

Sargent, W. L. W., Steidel, C. C., & Boksenberg, A. 1989, *ApJS*, 69, 703

Savage, B. D. & Jenkins, E. B. 1972, *ApJ*, 172, 491

Smith, H. E., Jura, M., & Margon, B. 1979, *ApJ*, 228, 369

Sorar, E. 1994, Ph.D. Thesis, Univ. Pittsburgh

Spitzak, J. G. & Schneider, S. E. 1998, *ApJS*, 119, 159

Steidel, C. C. & Sargent, W. L. W. 1992, *ApJS*, 80, 1 (SS92)

Storrie-Lombardi, L. J., Irwin, M. J., & McMahon, R. G. 1996a, *MNRAS*, 282, 1330

Storrie-Lombardi, L. J., McMahon, R. G., & Irwin, M. J. 1996b, *MNRAS*, 283, L79

Storrie-Lombardi, L. J., & Wolfe, A. M. 2000, *ApJ*, 543, 552

Turnshek, D. A., Wolfe, A. M., Lanzetta, K. M., Briggs, F. H., Cohen, R. D., Foltz, C. B., Smith, H. E., & Wilkes, B. J. 1989, *ApJ*, 344, 567

Turnshek, D. A., Rao, S. M., Nestor, D. B., Lane, W. M., Monier, E. M., Bergeron, J., & Smette, A. 2001, *ApJ*, 553, 288

Turnshek, D. A. & Rao, S. M. 2002, *ApJ*, 572, L7

Turnshek, D. A., Rao, S. M., Nestor, Vanden Berk, D., Belfort-Mihalyi, M., & Monier, E. M. 2004, *ApJ*, 609, L53

Turnshek, D. A., Rao, S. M., Nestor, D. B., Belfort-Mihalyi, M., & Quider, A. 2005, these proceedings

Tytler, D., Boksenberg, A., Sargent, W. L. W., Young, P., & Kunth, D. 1987, *ApJS*, 64, 667

Wagoner, R. 1967, *ApJ*, 149, 465

Weatherley, S. J., Warren, S. J., Møller, P., Fall, S. M., Fynbo, J. U., Croom, S. M. 2005, *MNRAS*, 358, 985

Weymann, R. J., Williams, R. E., Peterson, B. M., & Turnshek, D. A. 1979, *ApJ*, 234, 33

Wolfe, A. M., Turnshek, D. A., Smith, H. E., & Cohen, R. D. 1986, *ApJS*, 61, 249

Wolfe, A. M., Turnshek, D. A., Lanzetta, K. M., & Lu, L. 1993, *ApJ*, 404, 480

Wolfe, A. M., Lanzetta, K. M., Foltz, C. B., & Chaffee, F. H. 1995, *ApJ*, 454, 698

Wolfe, A. M., Gawiser, E., & Prochaska, J. X. 2003, *ApJ*, 593, 235

Wong, T. & Blitz, L. 2002, *ApJ*, 569, 157

Wright, A. E., Morton, D. C., Peterson, B. A., & Jauncey, D. L. 1979, *MNRAS*, 189, 611

Zwaan, M. A., Briggs, F. H., Sprayberry, D., & Sorar, E. 1997, *ApJ*, 490, 173

Zwaan, M. A., et al. 2003, *AJ*, 125, 2842

Zwaan, M. A., Meyer, M. J., Staveley-Smith, L., Webster, R. L. 2005, *MNRAS*, 359, 30

Discussion